Role of connexins in metastatic breast cancer and melanoma brain colonization

Konstantin Stoletov[1,2,*], Jan Strnadel[1,2,*], Erin Zardouzian[1,2], Masashi Momiyama[3,4], Frederick D. Park[1,2], Jonathan A. Kelber[1,2], Donald P. Pizzo[1,2], Robert Hoffman[3,4], Scott R. VandenBerg[1,2] and Richard L. Klemke[1,2,‡]

[1]Department of Pathology, University of California, San Diego, La Jolla, CA 92093, USA
[2]Moores Cancer Center, University of California, San Diego, La Jolla, CA 92093, USA
[3]Department of Surgery, University of California, San Diego, La Jolla, CA 92093, USA
[4]AntiCancer Inc., 7917 Ostrow St., San Diego, CA 92111, USA

*These authors contributed equally to this work
‡Author for correspondence (rklemke@ucsd.edu)

Accepted 11 December 2012
Journal of Cell Science 126, 904–913

doi: 10.1242/jcs.112748

Summary

Breast cancer and melanoma cells commonly metastasize to the brain using homing mechanisms that are poorly understood. Cancer patients with brain metastases display poor prognosis and survival due to the lack of effective therapeutics and treatment strategies. Recent work using intravital microscopy and preclinical animal models indicates that metastatic cells colonize the brain, specifically in close contact with the existing brain vasculature. However, it is not known how contact with the vascular niche promotes microtumor formation. Here, we investigate the role of connexins in mediating early events in brain colonization using transparent zebrafish and chicken embryo models of brain metastasis. We provide evidence that breast cancer and melanoma cells utilize connexin gap junction proteins (Cx43, Cx26) to initiate brain metastatic lesion formation in association with the vasculature. RNAi depletion of connexins or pharmacological blocking of connexin-mediated cell–cell communication with carbenoxolone inhibited brain colonization by blocking tumor cell extravasation and blood vessel co-option. Activation of the metastatic gene *twist* in breast cancer cells increased Cx43 protein expression and gap junction communication, leading to increased extravasation, blood vessel co-option and brain colonization. Conversely, inhibiting *twist* activity reduced Cx43-mediated gap junction coupling and brain colonization. Database analyses of patient histories revealed increased expression of Cx26 and Cx43 in primary melanoma and breast cancer tumors, respectively, which correlated with increased cancer recurrence and metastasis. Together, our data indicate that Cx43 and Cx26 mediate cancer cell metastasis to the brain and suggest that connexins might be exploited therapeutically to benefit cancer patients with metastatic disease.

Key words: Breast cancer metastasis, Brain metastasis, Connexins, Melanoma

Introduction

Approximately half of all cancer patients develop brain metastases leading to 20% of cancer-related deaths annually (Nussbaum et al., 1996; Lu et al., 2009). Breast and skin (melanoma) cancers are among the most common cancers that metastasize to the brain with about 10–20% of breast cancer patients and 40–60% of melanoma patients developing brain metastases. Patients with cancer metastasis to the brain have an extremely poor prognosis with less than ten months average survival time (Nussbaum et al., 1996; Lu et al., 2009). Treatment of brain cancer metastases is impeded by low permeability of the blood brain barrier to therapeutic agents, high sensitivity of brain tissue to irradiation, and the high number of advanced metastatic lesions at the time of diagnosis (Lu et al., 2009). Therefore, new molecular targets and therapeutic strategies that aim at brain metastatic lesions are sorely needed.

Although it is not clear why breast cancer and melanoma cells show a propensity to colonize the brain, brain micrometastases are initiated along the preexisting brain vasculature in close contact with the vessel surface (Kienast et al., 2010; Lorger and Felding-Habermann, 2010; Carbonell et al., 2009; Polyak and Weinberg, 2009). This suggests that the microenvironment of the vascular niche supports cancer cell survival and propagation during the early stages of brain colonization. However, the specific mechanisms used by metastatic cells to attach to the brain vasculature and propagate are poorly understood.

Connexin-mediated gap junctions (GJs) are strongly expressed in the vessel endothelium where they maintain vessel architecture and facilitate interactions with glial cells, which surround the vessel wall (Brisset et al., 2009; Figueroa and Duling, 2009). Glial cells play a key role in the maintenance of the blood–brain barrier by facilitating strong GJ-mediated adhesive interactions with the endothelium and by regulating heterocellular ion and small molecule transport activities (Simard et al., 2003; Balabanov and Dore-Duffy, 1998; Nagasawa et al., 2006; Haefliger et al., 2004). Similarly, metastatic tumors cells, which express connexins, may adhere to and propagate along the connexin-rich vasculature by forming heterotypic GJs with the endothelium and/or glia. Heterotypic GJ formation with stromal elements could also provide the means for the exchange of life sustaining ions and immunomodulatory factors, which are necessary to establish the tumor-cell–vascular niche and initiate microtumor formation. However, the role of connexins in mediating brain metastasis has not been defined and their role

Journal of Cell Science

in local and systemic cancer cell dissemination is controversial (reviewed by Laird, 2006; Naus and Laird, 2010).

Connexins have been reported to exhibit tumor-suppressor-like activities, to cause cancer cell dedifferentiation (mesenchymal to epithelial transition), and to inhibit metastasis (Laird et al., 1999; Naus and Laird, 2010; Ito et al., 2002). Also, mice with Cx43 inactivating mutations when crossed with the ErbB2 overexpressing mice show delayed onset of palpable mammary tumors while displaying increased pulmonary metastases (Plante et al., 2011). On the other hand, in melanoma, breast, and gastric cancers connexin 43 (Cx43) and 26 (Cx26) are upregulated in invasive lesions and in cells that disseminate to the lymph nodes (Naoi et al., 2007; Haass et al., 2010; Saito-Katsuragi et al., 2007; Elzarrad et al., 2008; Chao et al., 2012). Interestingly, high expression of Cx26 was detected in invasive, perivascular areas of primary melanomas, suggesting that heterotypic GJ-mediated cell–cell adhesion and communication contributes to melanoma metastasis (Haass et al., 2010; Saito-Katsuragi et al., 2007). Finally, metastatic breast cancer cells selected for their ability to home to the brain showed increased Cx43 expression (Bos et al., 2009). These findings lead one to believe that connexins may be differentially regulated during tumor cell dissemination. It is also possible that connexin expression may be restricted to distinct and rare tumor cell types that target specific organs like the brain, which is highly enriched in connexins. In any case, the conflicting data likely reflect the differences in experimental systems, the cellular heterogeneity of tumors, compensation by other connexin family members, and the complexity of the multi-step metastastic process in general. Reconciling these critical issues is important and warrants additional investigations. In this study, we examine the role of connexins Cx43 and Cx26 in mediating metastatic breast and melanoma cell brain colonization, respectively. For these studies, we use transparent zebrafish and chicken brain metastasis models combined with high-resolution fluorescence imaging methods to monitor the early events that initiate microtumor formation at the tumor-cell–vascular interface.

Results

Connexin expression in breast cancer and melanoma patients correlates with poor patient outcome

We first examined whether connexin expression in cancer patients correlates with patient prognosis and metastasis. We focused our attention on connexin isoforms 43 and 26, since they are the primary isoforms reported to be involved in breast cancer and melanoma metastasis (Elzarrad et al., 2008; Ito et al., 2002; Naoi et al., 2007; Haass et al., 2010; Saito-Katsuragi et al., 2007; Chao et al., 2012). To this end, we used the Oncomine (www.oncomine.org) cancer database that links various human gene expression profiles from primary and metastatic cancers to patient history. Although Oncomine did not specifically delineate cancer patients with brain metastases, it did reveal that increased Cx43 and Cx26 expression in primary breast cancer tumors correlated with poor patient survival and cancer recurrence (supplementary material Fig. S1A,B,H). In melanoma, increased Cx43 and 26 expression in primary lesions correlated with metastasis and poor patient survival (supplementary material Fig. S1C–G).

To determine the Cx43 expression pattern in established human brain metastases, we obtained rare brain metastases that had been surgically removed from four different breast cancer patients. In all four patients, Cx43 expression was significantly increased in the metastatic nodules compared to normal uninvolved brain tissue from the same patient sample (Fig. 1). However, the majority of Cx43 staining co-localized with the glial cell marker glial fibrillary acidic protein (GFAP). In fact, Cx43 immunoreactivity was not detected in the majority (>95%) of tumor cells present in the metastatic nodules, which are easily recognized by their large DAPI-stained nuclei and lack of GFAP expression (Fig. 1). Interestingly, close examination of the tumor-cell–vascular interface in metastatic nodules by

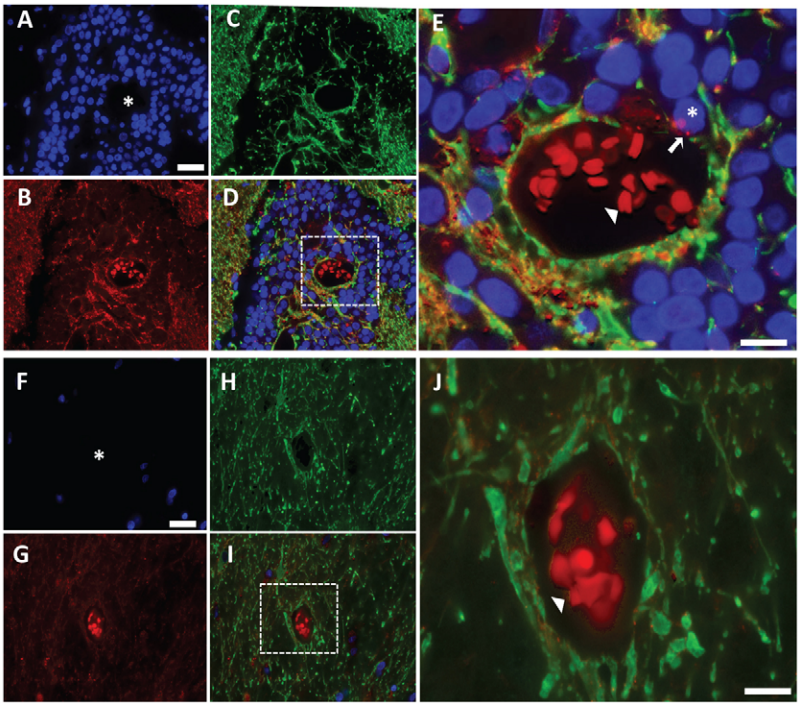

Fig. 1. Cx43 expression pattern in brain metastases from breast cancer patients. (**A–C**) Epifluorescent photomicrographs of a surgically resected brain metastasis from a breast cancer patient triple-stained for (A) nuclei (DAPI, blue), (B) Cx43 (red) and (C) the glial cell marker protein GFAP (green). (**D**) shows the merged images of A–C. (**E**) Zoomed region of box in D. Asterisk in A and the box in D show vessel lumen with autofluorescent red blood cells (red; arrowhead in E). Asterisk in E shows tumor on the vessel surface with positive Cx43 staining (arrow). (**F–I**) Epifluorescent photomicrographs of uninvolved normal brain tissue and associated blood vessel from the same brain metastasis specimen as above. (**J**) Zoomed region of box in I. Asterisk in F and the box in I show the vessel lumen with autofluorescent red blood cells (red; arrowhead in J). Scale bars: 25 µm (A,F), 10 µm (E,J).

high-resolution imaging revealed a small population (<5%) of Cx43-positive tumor cells contacting the blood vessel surface, which did not co-localize with GFAP (Fig. 1E). Although the patient sample size is small, these findings provide initial evidence that Cx43 expression might be restricted to a subpopulation of metastatic tumor cells in close association with the brain vasculature, which supports the notion that brain metastases develop in close proximity to the vasculature.

Metastatic 4T-1 breast cancer cells express Cx43 and form functional GJs with the endothelium

While microtumors develop in association with connexin-rich vasculature and stroma of the brain, the role of connexins in this process has not been examined (Kienast et al., 2010; Lorger and Felding-Habermann, 2010; Carbonell et al., 2009). To investigate this process, we first examined the ability of 4T-1 cancer cells to form GJs and transfer calcein orange dye to a monolayer of cultured EA.hy926 human endothelial cells *in vitro* (Bauer et al., 1992). 4T-1 is a well-studied mouse breast cancer cell line that readily metastasizes to the brain and other organs (Serres et al., 2012; Tao et al., 2008; Pulaski and Ostrand-Rosenberg, 2001). 4T-1 cells are known to express Cx43 and low levels of Cx26 (Fig. 2A), and they form functional GJs with cultured EA.hy926 cells (Fig. 2B). Importantly, inhibition of Cx43 expression in 4T-1 cells using 3–4 independent Cx43 shRNAs (4T-1KNCx43) (Fig. 2A,B) or siRNA (supplementary material Fig. S2A,B) prevented GJ communication with the endothelium. Interestingly, while loss of Cx43-mediated GJ communication did not impair 4T-1 cell growth under standard adherent culture conditions (Fig. 2C; supplementary material Fig. S2C), it did reduce 3D colony formation and the size of spheroids when cultured alone or co-cultured with endothelial cells (supplementary material Fig. S3A,B). Similar findings were also obtained using carbenoxolone (CBX), a reported GJ inhibitor (Farina et al., 1998) (Fig. 2B,C; supplementary material Fig. S2A–C, Fig. S3A,B). Together these demonstrate that 4T-1 cells form functional Cx43-mediated GJs with endothelial cells *in vitro* and this process is necessary for spheroid formation and colonization of 3D matrices.

Cx43 expression is required for metastatic breast cancer cell extravasation and blood vessel co-option in the brain

We next wanted to know if loss of Cx43 expression would impact brain colonization in preclinical animal models of brain metastasis. In mice, 4T-1KNCx43 cells showed significantly decreased ability to initiate microtumor formation in the brain compared to 4T-1 control cells after 3–7 days post injection into the carotid artery (Fig. 2D). We also used zebrafish and chicken embryo metastasis models since they are more amenable to visualizing initial events that mediate microtumor formation including cancer cell extravasation and vessel co-option using standard multi-color confocal microscopy (Stoletov et al., 2010; Stoletov et al., 2007; Zijlstra et al., 2002). In zebrafish, the majority (>90%) of 4T-1 cells quickly extravasated out of the brain vasculature, and invaded into the surrounding tissue (Fig. 3A,B). In contrast, 4T-1KNCx43 cells displayed significantly less extravasation potential than 4T-1 cells (Fig. 3A,B). Interestingly, 3-D imaging and morphometric shape analyses revealed that 36% of extravasated 4T-1 cells displayed an elongated invasive shape compared to only 8% of the 4T-1KNCx43 cells, which displayed a more rounded shape (Fig. 3C). This suggests that connexins may also be involved in mediating shape changes necessary for tissue invasion by breast cancer cells after their extravasation.

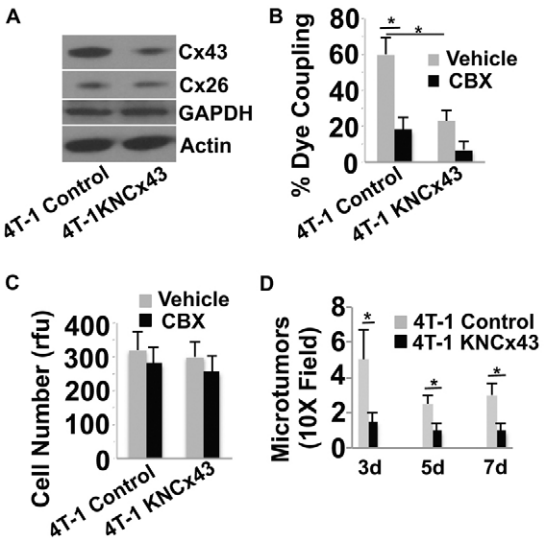

Fig. 2. Inhibition of Cx43 expression in breast cancer cells inhibits GJ communication *in vitro* and inhibits brain colonization in mice. (**A**). 4T-1 cells were either treated with an empty lentiviral vector (Control) or treated with the lentiviral vector encoding shRNA to Cx43 (4T-1KNcx43) to knock down Cx43 expression. Stable cells lines were then selected and Cx43 expression levels examined by western blotting. Actin, GAPDH and Cx26 served as specificity and loading controls. 4T-1KNcx43 cells show a 78% decrease in Cx43 expression compared with 4T-1 control cells, as measured by densitometry. (**B**) The indicated tumor cells were prelabeled with calcein orange dye and then added to a monolayer of EA.hy926 endothelial cells in the presence of the GJ inhibitor CBX (10 μM) or vehicle PBS. Dye transfer from tumor cells to endothelial cells was observed live by epifluorescence microscopy after 30 minutes of co-culture. The number of adherent cells that transferred dye to the adjacent endothelium was determined and represented as percentage of total number of tumor cells counted. (**C**) The indicated tumor cells were cultured *in vitro* and examined for cell growth for 3 days in the presence of CBX (10 μM) or vehicle using the CyQUANT assay. rfu, relative florescence units. (**D**) Average number of micrometastatic lesions in the mouse brain induced by 4T-1 and 4T-1KNcx43 cells at 3–7 days post injection. Data indicate means + s.e.m. *$P<0.05$.

The chicken metastasis model is beneficial in that it facilitates visualization and quantification of large numbers of tumor cells that have undergone extravasation and microtumor formation in the brain for up to 7 days post injection. While 4T-1 cells efficiently colonize the chicken brain, both 4T-1KNCx43 cells and 4T-1 siRNA cells depleted of Cx43 show significantly decreased brain colonization (Fig. 3D–F; supplementary material Fig. S2D). Importantly, many of the elongated 4T-1 cells grow along the brain vasculature closely contacting the vessel wall (Fig. 3D–F). These cells efficiently co-opt pre-existing brain vessels and form multiple metastatic microtumors, whereas, 4T-1KNCx43 cells show decreased vessel co-option, forming less and smaller metastatic lesions (Fig. 3D–F). Together, these findings indicate that Cx43 expression contributes to tumor cell extravasation and microtumor formation in association with the vasculature.

The metastatic gene *twist* induces Cx43 expression, tumor cell extravasation and brain colonization

Overexpression of the *twist* transcription factor in breast cancer and melanoma cells has been reported to increase cell metastasis

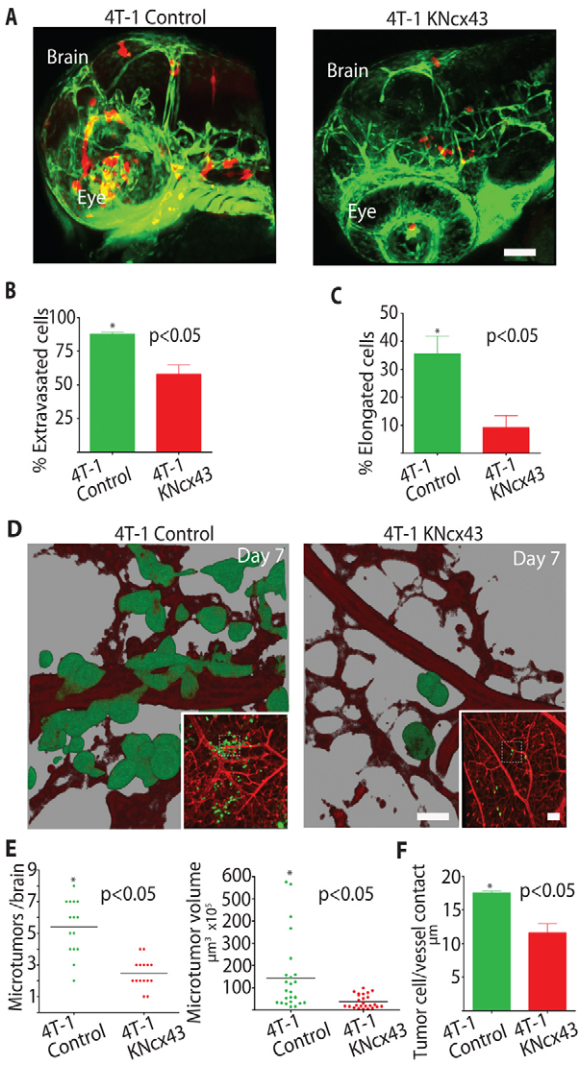

Fig. 3. Metastatic breast cancer cell extravasation and brain colonization require Cx43 expression. (**A**) 4T-1 control or 4T-1KNCx43 cells expressing dsRed were injected into the circulation of Tg(*fli1:egfp*) transgenic zebrafish and allowed to extravasate in the brain for 24 hours. Shown are representative 3D confocal reconstructions of the brain vasculature (green) and tumor cells (red) in the head region. (**B**) Average percentage of 4T-1 control and 4T-1KNcx43 cells that extravasated out of the vasculature into the brain parenchyma 24 hours after injection. (**C**) Average percentage of extravasated 4T-1 control and 4T-1KNCx43 cells with an elongated invasive morphology in the brain parenchyma. Scale bar: 200 µm. (**D**) 4T-1 control or 4T-1KNCx43 cells expressing GFP were injected into the chicken circulation and allowed to form microtumors in the brain for 7 days. Shown are representative 3D confocal reconstructions of the brain vasculature (red, Rhodamine–lectin stained) and tumor cells (green) (60×). Insets show lower magnification (10×); dashed squares indicate areas enlarged in the main panels. Note that 3D rendering shows that 4T-1 control cells co-opt brain blood vessels whereas 4T-1KNCx43 cells show little vessel association. (**E**) Number and volume of 4T-1 control and 4T-1KNCx43 microtumor lesions in the chicken brain after 7 days. (**F**) Average length of tumor-cell blood vessel contacts for 4T-1 control and 4T-1KNCx43 tumor cells after 7 days in the chicken brain. Scale bars: 20 µm (main panels), 200 µm (insets).

and correlate with poor patient prognosis (Yang et al., 2004; Mani et al., 2008; Elenbaas et al., 2001). However, it is not clear how twist induces tumor cell metastasis *in vivo*. Importantly, we found that *twist* overexpression in HMLE human breast cancer cells (HMLEtwist; Mani et al., 2008) induces increased expression of Cx43 protein (Fig. 4A,B). This was associated with increased Cx43-dependent GJ coupling to the endothelium *in vitro* (supplementary material Fig. S4A). The depletion of Cx43, or treatment with CBX did not significantly impact HMLE or HMLEtwist cell proliferation *in vitro* (supplementary material Fig. S4B). These findings demonstrate that expression of the metastatic gene *twist* induces Cx43 expression leading to increased GJ communication with the endothelium.

In zebrafish and chickens, HMLEtwist cells with increased Cx43 expression more rapidly extravasate and form more microtumors along the vessel surface compared to control HMLE cells without twist overexpression (Fig. 4A–C). These events required Cx43, as shRNA mediated knockdown of Cx43 expression in HMLEtwist cells (HMLEtwistKNCx43), inhibited cell extravasation and brain colonization (Fig. 4C–G). Also, in 4T-1 cells, shRNA mediated downregulation of endogenous *twist* expression (a mix of four or five independent shRNAs) resulted in robust relocalization of Cx43 from the cell membrane to the peri-nuclear region (Fig. 5A–C). This was associated with reduced GJ communication with the cultured endothelium (Fig. 5D). Inhibition of *twist* and Cx43 expression or treatment with CBX did not significantly impact 4T-1 cell proliferation in culture (Fig. 5E). Importantly, downregulation of endogenous *twist* expression did significantly decrease their ability of to colonize the chicken brain (Fig. 5F). These data indicate that twist facilitates breast cancer metastasis to the brain by increasing Cx43 expression and GJ communication with the endothelium.

Metastatic tumor cells form functional heterocellular GJs with the endothelium

The fact that metastatic breast cancer cells showed increased Cx43-dependent vessel co-option *in vivo* and GJ coupling to the endothelium *in vitro* suggest that successful metastatic cancer cells form heterocellular gap junctions with the brain endothelium *in vivo*. To investigate this possibility, we examined the ability of HMLEtwist and HMLEtwistKNCx43 cells to exchange calcein orange dye with the brain endothelium of live zebrafish (Laird, 2006; Saito-Katsuragi et al., 2007). HMLEtwist cells readily transfer calcein dye to the endothelium, whereas HMLEtwistKNCx43 cells did not indicating that dye transport required functional GJ communication and was not due to passive diffusion or cell lysis (supplementary material Fig. S5A,B). These findings suggest that cancer cells form functional GJs with brain endothelial cells in a Cx43-dependent manner.

Metastatic melanoma cells use Cx26 for brain perivascular microtumor formation

Similar to breast cancer, melanoma cells often metastasizes to the brain, prompting us to investigate if connexin-mediated tumor cell vessel co-option also plays a role in melanoma brain colonization. For these studies, we used an established mouse metastastic melanoma cell line (b16) that expresses Cx26, but not Cx43, and readily form functional GJs with the cultured endothelium in a Cx26 dependent manner (supplementary material Fig. S6A,B). b16 cells robustly colonized the chicken brain forming numerous microtumors that invade deep into the tissue along the preexisting vasculature (Fig. 6A). In contrast, b16 cells that were engineered to stably express Cx26-targeting shRNA constructs (b16KNcx26, mix of 4–5 independent

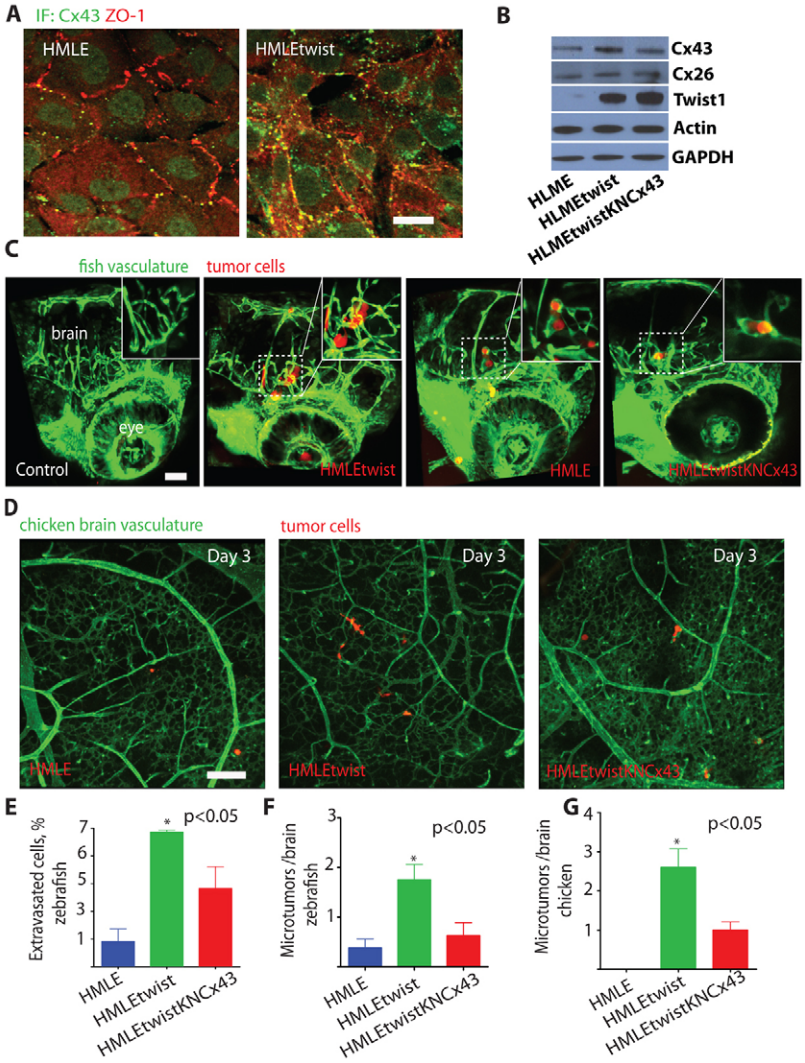

Fig. 4. Expression of the metastatic gene *twist* in breast cancer cells induces Cx43 expression, tumor cell extravasation and microtumor formation in the brain. (**A**) Representative images show 3D reconstructions of confocal z-stacks (60×, top views) of HMLE or HMLEtwist cell monolayers co-immunostained with Cx43 (green) and the cell–cell junction marker ZO-1 (red). (**B**) Western blots of the indicated proteins in HMLE cells transduced with the empty lentiviral vector (HLME), transduced with lenti-twist (HMLEtwist) or expressing twist and shRNAs to Cx43 (HMLEtwistKNCx43). HLMEtwist cells showed a 2.3-fold increase in Cx43 compared with HLME cells and HLMEtwistKNCx43 cells showed a 2.0-fold decrease compared with HLMEtwist cells, as measured by densitometry. (**C**) HMLE, HMLEtwist or HMLEtwistKNcx43 cells expressing dsRed were injected into the circulation of Tg(*fli1:egfp*) transgenic zebrafish and allowed to extravasate in the brain for 24 hours. Shown are representative 3D confocal reconstructions (20×) of the brain vasculature (green) and tumor cells (red) in the head region. The left-most panel shows 3D reconstruction of the head of a control, non-injected embryo. Insets show higher magnification (60×) of areas delineated by the dashed squares. (**D**) Brain microtumor formation of HMLE, HMLEtwist and HMLEtwistKNCx43 cells was assessed using the chicken metastasis assay. Representative 3D reconstructions (10×, top views) show confocal z-stacks of chicken embryo brains 3 days after intravenous injection of HMLE, HMLEtwist or HMLEtwistKNCx43 cells. (**E**) Average percentage of HMLE, HMLEtwist or HMLEtwistKNcx43 cells that extravasated in the zebrafish embryo brain 24 hours after injection. (**F**) Average number of microtumors per zebrafish brain induced by HMLE, HMLEtwist and HMLEtwistKNCx43 cells 24 hours after injection. (**G**) Average number of microtumors per chicken brain induced by HMLE, HMLEtwist and HMLEtwistKNCx43 cells 3 days after injection. Data indicate means + s.e.m. Scale bars: 20 μm (A) or 200 μm (C,D).

shRNAs) formed significantly less metastatic lesions, which were smaller and less invasive (Fig. 6B–D). These results show that in metastatic melanoma cells Cx26 expression enhances microtumor formation in the brain in association with the existing vasculature.

Survival of dormant, non-proliferating breast cancer cells involves connexin-mediated attachment to the brain vasculature

A major clinical problem in breast cancer is the inability to eradicate non-proliferating ‘dormant’ breast cancer cells (Nguyen et al., 2009; Chambers et al., 2002). For example, dormant breast cancer cells can reside undetected for many years in the brain before being activated to initiate cancer growth leading to patient relapse (Chambers et al., 2002; Goss et al., 2008). However, since these cells do not proliferate they cannot be targeted by conventional therapies (Goss et al., 2008). While the mechanisms that promote tumor cell dormancy are poorly understood, it is plausible that Cx43-mediated GJ communication with the vasculature is involved in this process (Kienast et al., 2010). Therefore, we investigated the role Cx43 in mediating the survival of dormant breast cancer cells in the brain using the dye retention model of cell dormancy (Kusumbe and Bapat, 2009). To visually monitor dormant breast cancer cells in the brain, GFP expressing 4T-1 breast cancer cells were labeled with PKH26 (red) membrane dye and imaged using confocal microscopy (Fig. 7A). Non-proliferating breast cancer cells retain the dye, while proliferating cells rapidly lose the dye after approximately three cell divisions (Kusumbe and Bapat, 2009). Using this approach, we found that the percentage of PKH26 positive 4T-1 cells rapidly declines within the first week post tumor cell injection (from 75% at day 1 post injection to 1.2% at day 7 post injection, Fig. 7B). In contrast, the percentage of PKH26 positive 4T-1 cells that remain in contact with the brain vasculature is increasing within the same period of time showing that non-proliferative dormant breast cancer cells require persistent association with the vasculature to survive (Fig. 7B). In contrast, less PKH positive 4T-1KNcx43 cells were seen contacting vessels in the brain compared to PKH positive 4T-1 cells at day 1 post injection. Importantly, the number of PKH positive 4T-1KNcx43 cells contacting vessels rapidly declined over the 6-day period (Fig. 7B). These data show that

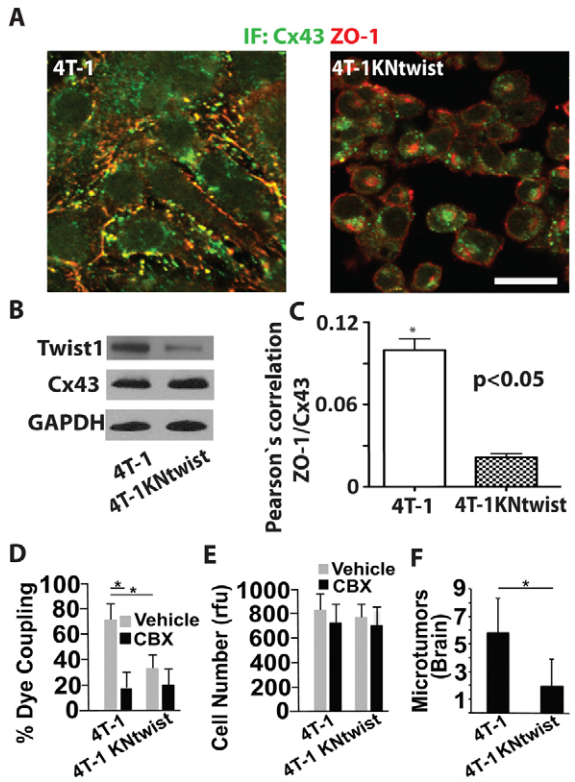

Fig. 5. Twist inhibition in metastatic breast cancer cells reduces Cx43-mediated GJ communication and inhibits brain microtumor formation. (**A**) Representative images show 3D reconstructions of confocal z-stacks (60×, top views) of 4T-1 expressing the empty lentiviral vector or 4T-1 cells expressing lentiviral vectors encoding shRNAs to *twist* (4T-1KNtwist). Cells were co-immunostained for Cx43 and ZO-1 and imaged as for Fig. 4A. Note that in cells with *twist* depleted, Cx43 is mostly intracellular, whereas ZO-1 is localized to the membrane. Scale bar: 20 µm. (**B**) Western blots of indicated proteins in 4T-1 and 4T-1KNtwist cells. Note that loss of twist expression inhibits membrane localization of Cx43 as shown in A, but not Cx43 total protein levels. 4T-1KNtwist cells show a 71% decrease in Twist1 expression compared to 4T-1 cells, as measured by densitometry. (**C**) Pearson's correlation analyses of Cx43 and ZO-1 colocalization in 4T-1 and 4T-1KNtwist cells immunostained as for A. (**D**) 4T-1 and 4T-1KNtwist cells in the presence of CBX (10 µM) or vehicle were examined for GJ-mediated calcein orange dye transfer to the cultured endothelium as described for Fig. 2B. (**E**) 4T-1 and 4T-1KNtwist cell growth in the presence of CBX (10 µM) or vehicle was determined as for Fig. 2C. (**F**) The number of 4T-1 and 4T-1KNtwist microtumors was assessed after 7 days in the chicken brain as described for Fig. 3D. Data indicate means + s.e.m. *$P<0.05$.

non-proliferative dormant metastatic breast cancer cells require contact with the vasculature to survive and that Cx43 is necessary for this process.

Pharmacological blocking of connexin-mediated cell–cell communication inhibits breast cancer and melanoma brain microtumor formation

CBX inhibits GJs, pannexins, and hemichannels and is a widely used to treat gastric ulceration and inflammation in humans (Juszczak and Swiergiel, 2009; Farina et al., 1998). It has also been successfully used intra-cranially in rats and mice to inhibit whole brain GJ communication and to alleviate post-traumatic pain suggesting that CBX could also be used to inhibit GJs in brain metastases (Khorasani et al., 2009; Juszczak et al., 2009; Roh et al., 2010). This and the fact that pharmacological compounds cross the blood–brain barrier in chickens prompted experiments to determine whether CBX treatment inhibited brain colonization and microtumor growth in the chicken brain metastasis model (Ribatti et al., 1993). Strikingly, we found that systemic delivery of CBX, but not vehicle, strongly decreased brain metastatic load of both 4T-1 breast cancer (Fig. 8A–D) and b16 melanoma cells (supplementary material Fig. S7A–D). CBX treatment also strongly inhibited the ability of 4T-1 breast cancer cells to contact the vasculature resulting in reduced number and size of 4T-1-induced brain microtumors (Fig. 8C,D). Similarly, CBX treatment decreased the number and size of b16 metastatic lesions associated with the vasculature (supplementary material Fig. S7C,D). Finally, CBX treatment inhibited the size and number of 4T-1 and b16 cells colonies that develop in a reconstituted 3D matrix *in vitro* (supplementary material Fig. S3A–D). Taken together, our findings suggest that connexin-mediated tumor-cell–vessel co-option and GJ communication could be a useful therapeutic mechanism to inhibit brain micrometastatic lesion progression.

Discussion

The role of connexins in cancer progression is controversial and not easily reconciled. Most likely this is due to cellular heterogeneity and the complex, multi-step, process of cancer development and progression. A substantial amount of work indicates that Cx43 expression is downregulated in primary breast cancer tumors. It is possible that the loss of GJ expression in primary tumor cells might be important for cells to physically detach from each other. During tumor progression, this could contribute to the local cell invasion into the surrounding stroma and vasculature, which are early steps in the metastatic process (Laird, 2006; Naus and Laird, 2010; Langlois et al., 2010). On the other hand, Cx43 and 26 were found to be upregulated in established breast cancer and melanoma metastatic lesions suggesting that connexins play roles in late metastatic steps involving vascular penetration and tissue colonization (Elzarrad et al., 2008; Ito et al., 2002; Naoi et al., 2007; Haass et al., 2010; Saito-Katsuragi et al., 2007; Chao et al., 2012). Also, the loss of connexins in primary tumor cells and its reemergence at metastatic sites suggest that connexin expression is dynamically regulated during cancer progression. In this regard, activation of the transcription factor twist is believed to be a late activating event that drives breast cancer and melanoma cell metastasis. We found that twist activation in cancer cells regulates Cx43 expression and its cellular localization, which is necessary for GJ coupling and brain colonization. This and the fact that Cx43 expression was necessary for tumor cell extravasation and microtumor formation is consistent with connexins contributing to late events in the metastatic cascade.

Connexins may also be expressed differentially in primary and disseminating tumor cells. For example, it is possible that connexin expression is restricted to minor populations of tumor cells endowed with invasive and cancer stem-cell-like properties (Lawson et al., 2009; Visvader and Lindeman, 2008). These migrating cancer stem cells are believed to be the metastatic culprits that seed secondary tissues. Interestingly, *twist* has been shown to promote a stem cell-like phenotype in breast cancer cells (Mani et al., 2008). Thus, it is possible that Cx43 expression is due in part to twist activation of a cancer stem cell program.

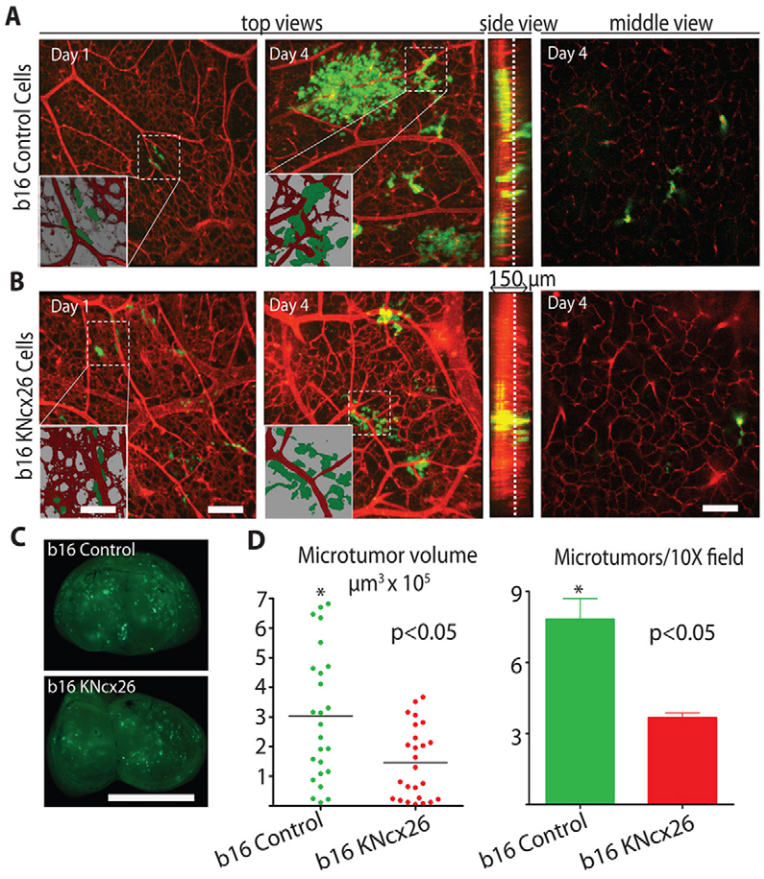

Fig. 6. Metastatic melanoma brain colonization requires Cx26. (**A**,**B**) b16 metastatic melanoma cells expressing the empty lentiviral vector (A; b16 control) or b16 cells stably expressing lentiviral shRNAs to Cx26 (B; b16KNcx26) along with GFP were injected into the chicken circulation and allowed to form microtumors in the brain for the indicated days. Top views are representative 3D confocal reconstructions of the brain vasculature (red, Rhodamine–lectin stained) and tumor cells (green) (60×). Insets show lower magnification (10×) of boxed areas. Note that 3D rendering shows that b16 control cells co-opt brain blood vessels whereas b16KNcx26 cells show little vessel association. Side view shows confocal z-stacks. Middle view shows representative optical slices from the middle of the z-stacks (slice positions indicated by the dashed lines in the side view). (**C**) Representative whole chicken brain images 4 days after intravenous injection of either b16 or b16KNCx26 cells, showing the level of brain colonization of GFP-labeled tumor cells. (**D**) Average volume and number of brain microtumors induced by b16 mock or b16KNCx26 cells 4 days after injection. Scale bars: 200 µm (A,B), 15 µm (A,B, inset), 0.5 cm (C).

Interestingly, connexin mediated cell–cell adhesion and communication have been shown to be involved in normal stem cell survival and proliferation (Todorova et al., 2008; Cheng et al., 2004; Wong et al., 2006). Also, human and mouse embryonic stem cells as well as human neural progenitors require GJ communication for their survival (Todorova et al., 2008; Cheng et al., 2004; Wong et al., 2006). Consistent with this idea we observed that only minor populations of Cx43-positive

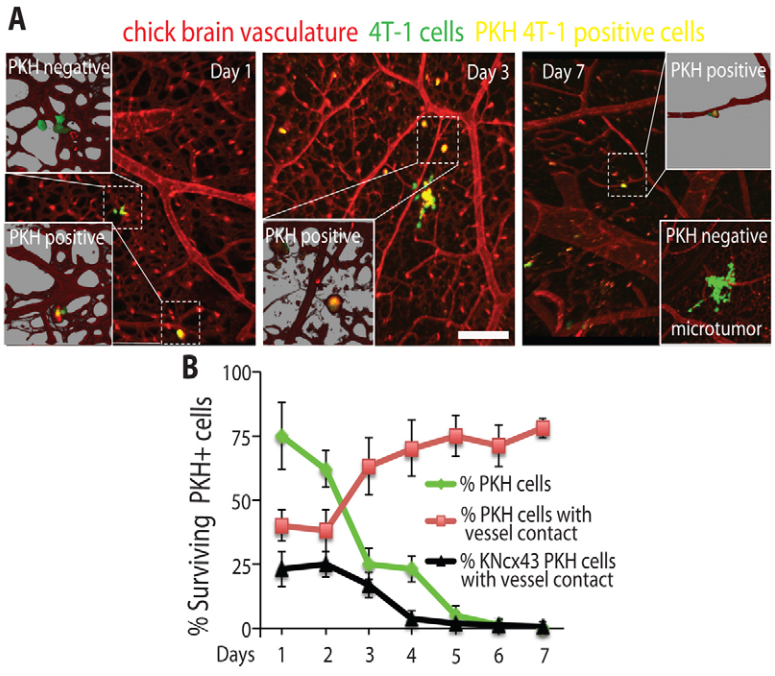

Fig. 7. Cx43 expression is necessary for survival of non-proliferating dormant breast cancer cells in the brain. (**A**) 4T-1 cells expressing GFP (green) and stained with the dye PKH26 (red) were injected into the chicken circulation and allowed to form microtumors in the brain for the indicated days. Confocal images were captured as described for Fig. 3D. Non-proliferating, dormant tumor cells retain PKH26 and appear yellow with the green GFP background. The chicken brain vasculature is labeled with Rhodamine–lectin (red). Insets show higher magnification of areas delineated by the dashed squares. Representative example of a PKH26-negative microtumor at day 7 post tumor cell injection is shown in the lower inset. (**B**) Average percentages of surviving PKH26-positive 4T-1 cells (green) or PKH26-positive 4T-1 (red) and 4T-1KNcx43 (black) cells that directly contact blood vessels in the chicken brain for the indicated days. Data indicate means ± s.e.m. Scale bar: 200 µm.

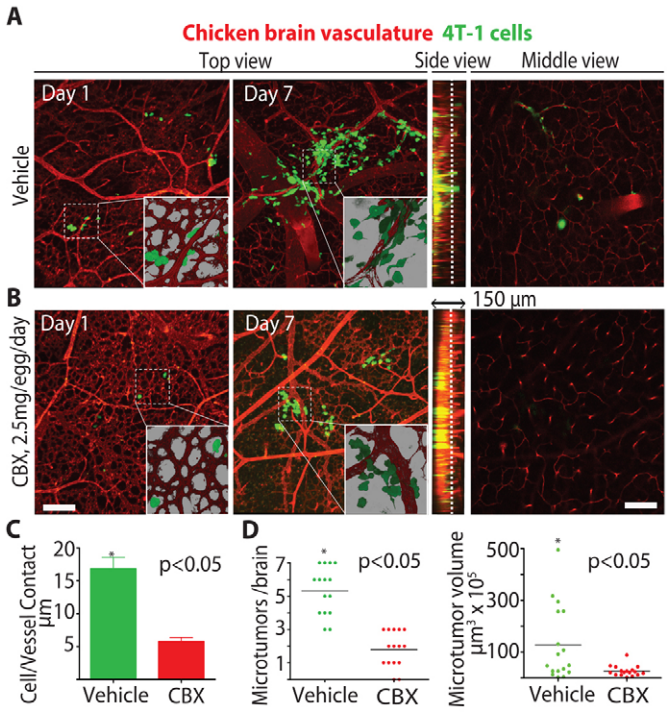

Fig. 8. The GJ inhibitor CBX inhibits breast cancer brain colonization. (**A**,**B**) Chickens were treated with (A) vehicle or (B) CBX (2.5 mg/egg/day) starting 1 day before tumor cell injection. Microtumor formation in the brain was assessed at the indicated days using confocal microscopy as described for Fig. 6B. Insets show higher magnification (60×) of the areas outlined by the dashed squares. The brain vasculature is labeled with Rhodamine–lectin dye (red). (**C**) Average length of tumor-cell blood vessel contacts for 4T-1 cells from the brains of vehicle or CBX-treated chicken 6 days after injection. (**D**) Number and volume of microtumors per chicken brain induced by 4T-1 tumor cells for vehicle or CBX-treated chickens 6 days after injection. Scale bars: 200 µm.

metastatic breast cancer cells reside in close proximity to the vascular system in the human brain (Fig. 1). Taken together our findings support the notion that connexins play a later role in regulating cancer progression rather than regulating early events in primary tumor development.

While we show that connexins are required for extravasation and microtumor growth in association with the brain vasculature their precise function in mediating these processes is not completely understood. As part of the extravasation process, connexins may mediate tumor cell adhesion and arrest in the brain vasculature using GJ-independent processes. For example, brain endothelial cell–cell junctions are highly enriched with Cx43, which could serve as homing sites for the attachment and extravasation of tumor cells expressing Cx43 (Haefliger et al., 2004). This might explain why breast and melanoma cells commonly metastasize to the brain. Indeed, Cx43 expression is increased in breast cancer cells selected for their propensity to metastasize to the brain (Bos et al., 2009).

It is intriguing that disseminating tumor cells do not completely arrest in the vessel, but migrate along the luminal surface in search of suitable sites to extravasate (Stoletov et al., 2010). Interestingly, Cx43 can regulate cell migration independent of its typical GJ functions (Olk et al., 2009). Increased Cx43-mediated intraluminal cell migration could contribute to the ability of tumor cells to survey and penetrate the vascular wall by forming heterotypic interactions with Cx43-rich endothelial cell–cell junctions.

Our findings suggest that traditional GJ-dependent mechanisms are also likely at play in forming brain metastases. For example, we show that extravasated tumor cells *in vivo* transfer dye to the brain endothelium in live animals and to cultured endothelial cells *in vitro* in a Cx43-dependent manner. Also, the GJ communication inhibitor, CBX, potently inhibited dye transfer and perivascular metastatic microtumor formation. These findings suggest that the transfer of ATP, critical ions, small peptides and even small regulatory RNAs through GJ channels could be crucial for tumor cell survival and growth after they leave the circulation (Laird, 2006; Mendoza-Naranjo et al., 2007; Katakowski et al., 2010). In this way, Cx43-mediated extravasation and heterocellular GJ formation with the Cx43-rich brain endothelium could facilitate tumor cell integration into foreign tissues creating a more hospitable niche for metastatic growth. The specific disruption of connexins using pharmaceuticals or genetic approaches could provide an efficient way to eradicate breast cancer and melanoma metastases in the brain.

Materials and Methods

Cell lines, cell culture, siRNA/shRNA constructs and antibodies

The human mammary carcinoma cell line HMLE and HMLEtwist (GFP or tomato red) were a generous gift from Dr Jing Yang (UCSD, Yang et al., 2004). Stable fluorescent mouse mammary cancer 4T-1 cells (GFP) were a generous gift from Dr David Schlaepfer (UCSD) and originally acquired from ATCC. Stable fluorescent b16 (GFP) mouse melanoma cell line was a generous gift from Dr Brunhilde Felding-Habermann (TSRI) and originally acquired from ATCC. Cells were cultured using standard conditions (www.atcc.org). Cx43 and 26 stable knockdown cell lines (HMLEtwistKNcx43) were generated using commercially available lentiviral vectors (Santa Cruz Biotechnology; sc-29276-V, sc-35091-V and sc-37051-V). Lentiviral particle production and infection were done according to the manufacturer recommendations. These lentiviral vectors consist of a pool of three to five plasmids designed to achieve maximum knockdown of target gene expression with minimum off target effects when expressed in the same cell. Control cells were established using the empty lentiviral vector. Knockdown was stable through at least 6 passages in culture as determined by western blotting. siRNA knockdown of Cx43 expression in tumor cells was performed using Cx43 siRNAs (sc-29276, according to the manufacturer's instructions. Scrambled siRNA (Santa Cruz Biotechnology) at the same concentration served as a control. Cells were used in experiments 48 hours after transfection. EA.hy926 endothelial cells were acquired from ATCC. Culturex 3D tumor-cell–endothelial co-culture was done as previously described (Barkan et al., 2008). Lab-Teck 8 well chamber slides (Fisher) were used for Culturex 3D culture using 2×10^4 cells per well for each experiment. For co-culture experiments 1:1 endothelial-tumor cell ratio was used. Cx43 antibody was from Cell Signaling (#3512) and GAPDH antibody was from AbCam (#ab22555).

Oncomine Analyses

Normalized gene expression signatures were collected using the gene summary viewer for several published breast cancer and melanoma patient arrays to assess the significance of Cx43 and Cx26 gene expression on disease progression and patient outcome. Data was plotted as an average, with a minimum and maximum measurement for each patient group.

Tumor cell to endothelial cell dye transfer

Tumor cells (1×10^6 cells/ml) were preloaded with 30 µM of the cell permeable calcein red–orange dye (#C3481, Life Technologies) for 30 minutes in suspension using standard tissue culture conditions. Cells were then rinsed with PBS and resuspended in culture media (1×10^5 cells/ml) prior to experiments with CBX (10 µM, Sigma) or vehicle. Labeled tumor cells (1000) were added to a confluent monolayer of EA.hy926 endothelial cells on Lab-Tek 8 well glass bottom chamber slides (Fisher) in the continued presence of 10 µM CBX or vehicle. Cells were allowed to adhere for 30 minutes before dye transfer from tumor cells to the adjacent endothelium was captured using live-cell epifluorescence microscopy. The number of adherent cells that transferred dye to adjacent endothelial cells was recorded and expressed as percent of the total number of tumor cells counted. For

each chamber, 40–60 attached cells were recorded. All experiments were repeated twice with triplicate chambers.

Mouse brain metastasis model

Animals were maintained according to the University of California San Diego animal welfare guidelines, as described and approved UCSD Institutional Animal Care and Use Committee (S99001). Athymic NCR nude mice (nu/nu), 5–6 weeks of age were used for the study. The breeding pairs were obtained from Charles River Laboratories (Wilmington, MA). Mice were kept in a barrier facility under HEPA filtration and fed with autoclaved laboratory rodent diet. Mice were anesthetized with a ketamine mixture (10 µl ketamine HCL, 7.6 µl xylazine, 2.4 µl acepromazine maleate, and 10 µl H_2O) via s.c. injection. The carotid artery was exposed by blunt dissection and 2.5×10^5 GFP-labeled 4T-1KNcx43 or mCherry-labeled 4T-1 parental cells were injected into the right internal carotid artery. The skin was closed with a 6-0 surgical suture (ETHICON, Inc.) and 3–7 days later, injected animals were euthanized using CO_2 exposure, their brains were removed and GFP/mCherry positive microtumors localized and counted using using Nikon c1-si confocal microscope, a 10× objective, and Imaris software. At least three animals were used for each experiment.

Zebrafish cancer cell extravasation assay

Animals were maintained according to the University of California San Diego animal welfare guidelines as described and approved by UCSD Institutional Animal Care and Use Committee and protocol number S06008 (Nusslein-Volhard and Dahm, 2002). Zebrafish extravasation assay was done as previously described (Stoletov et al., 2010). Briefly, Zebrafish embryos were obtained using standard mating conditions and staged by hours post fertilization (hpf). At 48 hpf, embryos were de-chorionized and anesthetized with tricaine. 200–300 human tumor cells in 50 nl of PBS were injected into the common cardinal vein using an Eppendorf FemtoJet injector. Embryos that contain brain-arrested cells were imaged using Nikon c1-si confocal microscope, and the percentage of extravasated cells outside the vasculature was quantified as previously described (Stoletov et al., 2010). At least 10 animals were used for each experiment.

Western blotting

Cell extracts were prepared in SDS buffer containing complete protease inhibitor cocktail. Protein concentrations were determined by bicinchoninic acid assay (Pierce). Equal amounts of cell extracts were resolved by SDS-PAGE, electrotransferred to PVDF membranes, and probed with primary antibodies.

Immunofluorescence of cells and human brain breast cancer metastases

Cells were plated on Lab-Tek 8 chamber glass coverslips (Fisher), fixed in 4% formaldehyde, permeabilized in 0.2% Triton X-100, and incubated with anti-Cx43 or ZO-1 antibodies (1:100) followed by secondary antibodies conjugated with Alexa Fluor 488 or Alexa Fluor 594 (Molecular Probes). Coverslips were mounted using ProLong Gold (Invitrogen) mounting media and imaged using a Nikon C1-si confocal microscope. Images were obtained using a 60× oil immersion objective and analyzed using Imaris imaging software.

Breast cancer brain metastasis tissue samples from four patients were obtained from UCSD Moores Cancer Center Tissue Repository. Tissue sections were cut from blocks of formalin-fixed paraffin tumor tissue of UCSD patients that had metastatic breast cancer to the brain. Four-micron tissue sections were stained with a rabbit polyclonal antibody to Cx43 (#3512, Cell Signaling Technology, Inc.), and a mouse monoclonal antibody to GFAP (E16510, Spring Bioscience) using Discovery Ultra (Ventana Medical Systems). Antigen retrieval was performed using CC1 for 24 minutes at 95℃. Primary antibodies were used at 1:150 dilution for Cx43 and 1:600 dilution for GFAP for 1 hour at 37℃ followed by fluorescently labeled (donkey anti-rabbit 594; donkey anti-mouse 488) secondary antibodies (Jackson ImmunoResearch) at 1:750 dilution for 60 minutes. Slides were rinsed, and coverslipped (Prolong Gold with DAPI, Invitrogen). Slides were visualized on a Zeiss Axio Imager2 using Cambridge Research Instruments (CRi) Nuance Multispectral Imaging System software to capture the images and unmix pure spectra. Using this software, a pure fluorophore spectrum is acquired and then compared to a complex mixture of spectrum, which includes autofluorescence. Individual fluorophore spectrum as well as autofluorescence can be individually displayed.

Chicken embryo cancer metastasis assay

Fertilized chicken eggs were purchased from McIntire Poultry (Lakeside, CA) and incubated for 14 days (37℃, 100% humidity). A 1 cm^2 square window was created in the eggshell to expose the underlying vasculature. Tumor cells were suspended in sterile PBS at the concentration of 2×10^6 cells/ml and 2×10^5 tumor cells (100 µl/embryo) were injected into the main CAM vein. After incubating embryos for another 1–7 days, Rhodamine-lectin (Vector Biolabs; 100 µl/embryo, 0.5 mg/ml) was injected into the CAM vein. Following appropriate euthanizing procedures, the chicken brain and liver were removed and imaged using either Leica MZFLIII microscope (1.25×) or Nikon c1-si confocal microscope (10–60×). CBX (10 mg/ml in PBS) (Sigma) was injected into the chicken embryo amniotic fluid 2.5 mg/embryo/day. CBX treatment led to ~30% decrease in the embryo survival however no gross organ or tissue morphology effects were observed. Cancer dormancy and PKH membrane dye (Sigma) staining was performed as according to the manufactures recommendation and as previously described (Kusumbe and Bapat, 2009).

Statistical analysis

All data were analyzed using unpaired Student's *t*-test built into the GraphPad Prizm software (www.graphpad.com) for statistical significance. Data plots show mean values ± s.e.m.

Acknowledgements

We would like to thank Sandra Walsh, President of California Breast Cancer Organizations and Nancy Tavolazzi for breast cancer advocate support of the project. We thank Dr Jing Yang (University of California San Diego) for providing HMLE and HMLEtwist cells, Dr David Schlaepfer (University of California San Diego) for providing 4T-1 cells and Dr Brunhilde Felding-Habermann (The Scripps Research Institute) for providing b16 cells.

Author contributions

K.S., J.S., E.Z., M.M., F.D.P., J.A.K. and D.P.P. performed the experiments. R.H. and S.R.V. assisted with manuscript preparation and data analysis. R.L.K. performed data analysis and wrote the manuscript.

Funding

This work was supported by the National Institutes of Health [grant numbers CA097022, GM064346 to R.L.K.]. Deposited in PMC for release after 12 months.

Supplementary material available online at
http://jcs.biologists.org/lookup/suppl/doi:10.1242/jcs.112748/-/DC1

References

Balabanov, R. and Dore-Duffy, P. (1998). Role of the CNS microvascular pericyte in the blood-brain barrier. *J. Neurosci. Res.* **53**, 637-644.

Barkan, D., Kleinman, H., Simmons, J. L., Asmussen, H., Kamaraju, A. K., Hoenorhoff, M. J., Liu, Z. Y., Costes, S. V., Cho, E. H., Lockett, S. et al. (2008). Inhibition of metastatic outgrowth from single dormant tumor cells by targeting the cytoskeleton. *Cancer Res.* **68**, 6241-6250.

Bauer, J., Margolis, M., Schreiner, C., Edgell, C. J., Azizkhan, J., Lazarowski, E. and Juliano, R. L. (1992). In vitro model of angiogenesis using a human endothelium-derived permanent cell line: contributions of induced gene expression, G-proteins, and integrins. *J. Cell. Physiol.* **153**, 437-449.

Bos, P. D., Zhang, X. H., Nadal, C., Shu, W., Gomis, R. R., Nguyen, D. X., Minn, A. J., van de Vijver, M. J., Gerald, W. L., Foekens, J. A. et al. (2009). Genes that mediate breast cancer metastasis to the brain. *Nature* **459**, 1005-1009.

Brisset, A. C., Isakson, B. E. and Kwak, B. R. (2009). Connexins in vascular physiology and pathology. *Antioxid. Redox Signal.* **11**, 267-282.

Carbonell, W. S., Ansorge, O., Sibson, N. and Muschel, R. (2009). The vascular basement membrane as "soil" in brain metastasis. *PLoS ONE* **4**, e5857.

Chambers, A. F., Groom, A. C. and MacDonald, I. C. (2002). Dissemination and growth of cancer cells in metastatic sites. *Nat. Rev. Cancer* **2**, 563-572.

Chao, Y., Wu, Q., Acquafondata, M., Dhir, R. and Wells, A. (2012). Partial mesenchymal to epithelial reverting transition in breast and prostate cancer metastases. *Cancer Microenviron.* **5**, 19-28.

Cheng, A., Tang, H., Cai, J., Zhu, M., Zhang, X., Rao, M. and Mattson, M. P. (2004). Gap junctional communication is required to maintain mouse cortical neural progenitor cells in a proliferative state. *Dev. Biol.* **272**, 203-216.

Elenbaas, B., Spirio, L., Koerner, F., Fleming, M. D., Zimonjic, D. B., Donaher, J. L., Popescu, N. C., Hahn, W. C. and Weinberg, R. A. (2001). Human breast cancer cells generated by oncogenic transformation of primary mammary epithelial cells. *Genes Dev.* **15**, 50-65.

Elzarrad, M. K., Haroon, A., Willecke, K., Dobrowolski, R., Gillespie, M. N. and Al-Mehdi, A. B. (2008). Connexin-43 upregulation in micrometastases and tumor vasculature and its role in tumor cell attachment to pulmonary endothelium. *BMC Med.* **6**, 20.

Farina, C., Pinza, M. and Pifferi, G. (1998). Synthesis and anti-ulcer activity of new derivatives of glycyrrhetic, oleanolic and ursolic acids. *Farmaco.* **53**, 22-32.

Figueroa, X. F. and Duling, B. R. (2009). Gap junctions in the control of vascular function. *Antioxid. Redox Signal.* **11**, 251-266.

Goss, P., Allan, A. L., Rodenhiser, D. I., Foster, P. J. and Chambers, A. F. (2008). New clinical and experimental approaches for studying tumor dormancy: does tumor dormancy offer a therapeutic target? *APMIS* **116**, 552-568.

Haass, N. K., Ripperger, D., Wladykowski, E., Dawson, P., Gimotty, P. A., Blome, C., Fischer, F., Schmage, P., Moll, I. and Brandner, J. M. (2010). Melanoma progression exhibits a significant impact on connexin expression patterns in the epidermal tumor microenvironment. *Histochem. Cell Biol.* **133**, 113-124.

Haefliger, J. A., Nicod, P. and Meda, P. (2004). Contribution of connexins to the function of the vascular wall. *Cardiovasc. Res.* **62**, 345-356.

Ito, A., Watabe, K., Koma, Y. and Kitamura, Y. (2002). An attempt to isolate genes responsible for spontaneous and experimental metastasis in the mouse model. *Histol. Histopathol.* **17**, 951-959.

Juszczak, G. R. and Swiergiel, A. H. (2009). Properties of gap junction blockers and their behavioural, cognitive and electrophysiological effects: animal and human studies. *Prog. Neuropsychopharmacol. Biol. Psychiatry* **33**, 181-198.

Katakowski, M., Buller, B., Wang, X., Rogers, T. and Chopp, M. (2010). Functional microRNA is transferred between glioma cells. *Cancer Res.* **70**, 8259-8263.

Khorasani, M. Z., Hosseinzadeh, S. A. and Vakili, A. (2009). Effect of central microinjection of carbenoxolone in an experimental model of focal cerebral ischemia. *Pak. J. Pharm. Sci.* **22**, 349-354.

Kienast, Y., von Baumgarten, L., Fuhrmann, M., Klinkert, W. E., Goldbrunner, R., Herms, J. and Winkler, F. (2010). Real-time imaging reveals the single steps of brain metastasis formation. *Nat. Med.* **16**, 116-122.

Kusumbe, A. P. and Bapat, S. A. (2009). Cancer stem cells and aneuploid populations within developing tumors are the major determinants of tumor dormancy. *Cancer Res.* **69**, 9245-9253.

Laird, D. W. (2006). Life cycle of connexins in health and disease. *Biochem. J.* **394**, 527-543.

Laird, D. W., Fistouris, P., Batist, G., Alpert, L., Huynh, H. T., Carystinos, G. D. and Alaoui-Jamali, M. A. (1999). Deficiency of connexin43 gap junctions is an independent marker for breast tumors. *Cancer Res.* **59**, 4104-4110.

Langlois, S., Cowan, K. N., Shao, Q., Cowan, B. J. and Laird, D. W. (2010). The tumor-suppressive function of Connexin43 in keratinocytes is mediated in part via interaction with caveolin-1. *Cancer Res.* **70**, 4222-4232.

Lawson, J. C., Blatch, G. L. and Edkins, A. L. (2009). Cancer stem cells in breast cancer and metastasis. *Breast Cancer Res. Treat.* **118**, 241-254.

Lorger, M. and Felding-Habermann, B. (2010). Capturing changes in the brain microenvironment during initial steps of breast cancer brain metastasis. *Am. J. Pathol.* **176**, 2958-2971.

Lu, J., Steeg, P. S., Price, J. E., Krishnamurthy, S., Mani, S. A., Reuben, J., Cristofanilli, M., Dontu, G., Bidaut, L., Valero, V. et al. (2009). Breast cancer metastasis: challenges and opportunities. *Cancer Res.* **69**, 4951-4953.

Mani, S. A., Guo, W., Liao, M. J., Eaton, E. N., Ayyanan, A., Zhou, A. Y., Brooks, M., Reinhard, F., Zhang, C. C., Shipitsin, M. et al. (2008). The epithelial-mesenchymal transition generates cells with properties of stem cells. *Cell* **133**, 704-715.

Mendoza-Naranjo, A., Saéz, P. J., Johansson, C. C., Ramírez, M., Mandakovic, D., Pereda, C., López, M. N., Kiessling, R., Sáez, J. C. and Salazar-Onfray, F. (2007). Functional gap junctions facilitate melanoma antigen transfer and cross-presentation between human dendritic cells. *J. Immunol.* **178**, 6949-6957.

Nagasawa, K., Chiba, H., Fujita, H., Kojima, T., Saito, T., Endo, T. and Sawada, N. (2006). Possible involvement of gap junctions in the barrier function of tight junctions of brain and lung endothelial cells. *J. Cell. Physiol.* **208**, 123-132.

Naoi, Y., Miyoshi, Y., Taguchi, T., Kim, S. J., Arai, T., Tamaki, Y. and Noguchi, S. (2007). Connexin26 expression is associated with lymphatic vessel invasion and poor prognosis in human breast cancer. *Breast Cancer Res. Treat.* **106**, 11-17.

Naus, C. C. and Laird, D. W. (2010). Implications and challenges of connexin connections to cancer. *Nat. Rev. Cancer* **10**, 435-441.

Nguyen, D. X., Bos, P. D. and Massagué, J. (2009). Metastasis: from dissemination to organ-specific colonization. *Nat. Rev. Cancer* **9**, 274-284.

Nussbaum, E. S., Djalilian, H. R., Cho, K. H. and Hall, W. A. (1996). Brain metastases. Histology, multiplicity, surgery, and survival. *Cancer* **78**, 1781-1788.

Nusslein-Volhard, C. and Dahm, R. (2002). *Zebrafish: a Practical Approach*. Oxford: Oxford University Press.

Olk, S., Zoidl, G. and Dermietzel, R. (2009). Connexins, cell motility, and the cytoskeleton. *Cell Motil. Cytoskeleton* **66**, 1000-1016.

Plante, I., Stewart, M. K., Barr, K., Allan, A. L. and Laird, D. W. (2011). Cx43 suppresses mammary tumor metastasis to the lung in a Cx43 mutant mouse model of human disease. *Oncogene* **30**, 1681-1692.

Polyak, K. and Weinberg, R. A. (2009). Transitions between epithelial and mesenchymal states: acquisition of malignant and stem cell traits. *Nat. Rev. Cancer* **9**, 265-273.

Pulaski, B. A. and Ostrand-Rosenberg, S. (2001). Mouse 4T1 breast tumor model. *Curr. Protoc. Immunol.* **Chapter 20**, Unit 20.2.

Ribatti, D., Nico, B. and Bertossi, M. (1993). The development of the blood-brain barrier in the chick. Studies with evans blue and horseradish peroxidase. *Ann. Anat.* **175**, 85-88.

Roh, D. H., Yoon, S. Y., Seo, H. S., Kang, S. Y., Han, H. J., Beitz, A. J. and Lee, J. H. (2010). Intrathecal injection of carbenoxolone, a gap junction decoupler, attenuates the induction of below-level neuropathic pain after spinal cord injury in rats. *Exp. Neurol.* **224**, 123-132.

Saito-Katsuragi, M., Asada, H., Niizeki, H., Katoh, F., Masuzawa, M., Tsutsumi, M., Kuniyasu, H., Ito, A., Nojima, H. and Miyagawa, S. (2007). Role for connexin 26 in metastasis of human malignant melanoma: communication between melanoma and endothelial cells via connexin 26. *Cancer* **110**, 1162-1172.

Serres, S., Soto, M. S., Hamilton, A., McAteer, M. A., Carbonell, W. S., Robson, M. D., Ansorge, O., Khrapitchev, A., Bristow, C., Balathasan, L. et al. (2012). Molecular MRI enables early and sensitive detection of brain metastases. *Proc. Natl. Acad. Sci. USA* **109**, 6674-6679.

Simard, M., Arcuino, G., Takano, T., Liu, Q. S. and Nedergaard, M. (2003). Signaling at the gliovascular interface. *J. Neurosci.* **23**, 9254-9262.

Stoletov, K., Montel, V., Lester, R. D., Gonias, S. L. and Klemke, R. (2007). High-resolution imaging of the dynamic tumor cell vascular interface in transparent zebrafish. *Proc. Natl. Acad. Sci. USA* **104**, 17406-17411.

Stoletov, K., Kato, H., Zardouzian, E., Kelber, J., Yang, J., Shattil, S. and Klemke, R. (2010). Visualizing extravasation dynamics of metastatic tumor cells. *J. Cell Sci.* **123**, 2332-2341.

Tao, K., Fang, M., Alroy, J. and Sahagian, G. G. (2008). Imagable 4T1 model for the study of late stage breast cancer. *BMC Cancer* **8**, 228.

Todorova, M. G., Soria, B. and Quesada, I. (2008). Gap junctional intercellular communication is required to maintain embryonic stem cells in a non-differentiated and proliferative state. *J. Cell. Physiol.* **214**, 354-362.

Visvader, J. E. and Lindeman, G. J. (2008). Cancer stem cells in solid tumours: accumulating evidence and unresolved questions. *Nat. Rev. Cancer* **8**, 755-768.

Wong, R. C., Dottori, M., Koh, K. L., Nguyen, L. T., Pera, M. F. and Pébay, A. (2006). Gap junctions modulate apoptosis and colony growth of human embryonic stem cells maintained in a serum-free system. *Biochem. Biophys. Res. Commun.* **344**, 181-188.

Yang, J., Mani, S. A., Donaher, J. L., Ramaswamy, S., Itzykson, R. A., Come, C., Savagner, P., Gitelman, I., Richardson, A. and Weinberg, R. A. (2004). Twist, a master regulator of morphogenesis, plays an essential role in tumor metastasis. *Cell* **117**, 927-939.

Zijlstra, A., Mellor, R., Panzarella, G., Aimes, R. T., Hooper, J. D., Marchenko, N. D. and Quigley, J. P. (2002). A quantitative analysis of rate-limiting steps in the metastatic cascade using human-specific real-time polymerase chain reaction. *Cancer Res.* **62**, 7083-7092.

Journal of Cell Science